[19] Wilson, L.L., Joseph C. Foster Jr., S.E. Jones and Peter P. Gillis, **"Experimental Rod Impact Results"**, Int. J. Impact Engng. Vol.8, pp. 15-25 (1989).

[20] Dehn, J., **"A Unified Theory of Penetration"**, Int. J. Impact Engng. Vol.5, pp. 238-248 (1987).

[21] Anderson Charles E., and S.R. Bonder, **"Ballistic Impact: The Status of Analytical and Numerical Modeling"**, Int. J. Impact Engng. Vol.7, No.1, pp 9-35 (1988).

[22] Wilkins, M.L, **"Mechanics of Perforation and Penetration"**, Int. J. Engng. Sci. Vol. 16, pp. 1-76 (1987).

[23] Wilkins, M.L., and M.W. Guinan, **"impact of Cylinders on a Rigid Boundary"**, J. Appl. Phys. Vol. 44, pp. 1200-1206 (1973).

[24] Sedgwick, R.T., L.G. Hageman, R.G. Herrmann, and J.L. Waddell, **Numerical Investigations in Penetration Mechanics**, Int. J. Engng. Sci. 16, 859-870 (1978).

[25] Bertholf, L.D., L.D. Buxton, B.J. Thorne, R.K. BYERS, A.L Stevens and S.L. Thompson, **"Damage In Steel Plates From Hypervelocity Impact- II: Numerical Results and Spall Measurement"**, J. Appl. Phys. Vol. 46, pp. 377-3783 (1975).

[26] Kleinbaum, D.G and Kupper Lawrence L., **Applied Regression Analysis and Other Multivariable Methods"**, Wadsworth Publishing Company, (1978).

[27] Walpole, R.E. and Myers H.R., **"Probability and Statistics for Enginners and Scientists"**, Macmillan Book Company (1978).

[28] Green, K.B., and P.G. Ghamberlain, **"Model Scale Experiments on Long Rod Penetration"**. Maryland: U.S. Army, Ballistic Research Laboratory, (1980).

[29] Blanks, James R., **"Penetration Test of Semi- Infinite Steel Targets by Tungsten Alloy Rods"**, AEDC- TSR- 83- V26, Calspan Fiedls Services, Inc., September 1983, (Plus Data Package).

[30] B.R. Sorensen, K.D. Kimsey, G.F. Silsby, D.R. Scheffelr, T.M. Sherrick and W.S. De Rosset. **"High Velocity Penetration of Steel Targets"** Int. J. Impact Engng. Vol. 11, No.1, pp. 107-119, (1991).

formulation and the relationship between u and v may require more development. In the case of resistance expression more accurate representation of resistive pressure requires considerations of strain rate and strain hardening effects which leads to metallurgical consideration of yield strength.

References

[1] Zukas, J.A., T. Nicholas, H.F. Swift, L.B. Greszezuk, and D.R. clurren, **"Impact Dynamics"**, Wiley- Interscience, New York (1982).

[2] Billington, E.W., and A. Tate, "physics of Deformation and Flow, McGraw- Hill Book Co., New York, pp. 509-540 (1982).

[3] Wright, T.W **"A Survey Of Penetration Mechanics for Long Rods"**, In Lecture Notes in Engineering, Vol.3, **"Computational Aspect of Penetration Mechanics"** (edited by J. Chandra and J. Flaherty), pp. 85-106 Springer- Verlag, New York (1983).

[4] Recht, R.F. and T.W. Ipson, **"Ballistic Perforation Dynamics"**, J. Appl. Mech. Vol. 30, pp. 384-390 (1963).

[5] Grabarek C. **"Penetration of Armor by Steel and High Density Penetrators"**, Ballistic Research Laboratory BRL- MR- 2134, AD 518394L (1971).

[6] Backman, M.E. and Goldsmith, W., **"The Mechanics of Penetration of Projectiles into Targets"**, Int. J. Engng. Sci. Vol. 16, pp. 1-99 (1978).

[7] Birkhoff, G., D. MacDougall, E., Pugh and G. Taylor. "Explosives **with Lined Cavities**, Vol. 19, J. App. Phys (1948).

[8] Echelberger, R.J. **"Experimental Test of the Theory of Penetration by the Metallic Jets2"**, J. Appl. Phys. Vol.27, pp. 63-68 (1956).

[9] Sternberg Joseph, **"A Critical Review of Target Strength Effect in Resisting High Velocity Penetration"**, RDA Logicon R & D Associates, DARPA Sponsorhsip, Contract: DNA- 001-84- c- 0314, (Oct 1985).

[10] William P. Walters, and J.A. Zukas, **"Fundamental of Shaped Charges"**, Wiley-Interscience, (1989).

[11] William P. Walters, W.J. Fils, and P.C. Chou. **"A Survey of the Shaped Charge Jet Penetration Models"**, Int J. Impact Engng. Vol. 7, No.3, pp. 3-7-325, (1988).

[12] Ravid, M., S.R. Bonder and I. Holcman, **"Analysis of Very Highh Speed Impact"**, Int. J. Engng Sci, Vol. 25, pp. 473-482 (987).

[13] Allen, W.A. and J.W. Rogers, **"Penetration of Rods into a Semi- Infinite Target"**, J. Franklin Inst., Vol. 272, pp. 257-284 (1961).

[14] Christman, D.R. and J.W. Gehring, **"Analysis of High Velocity Projectiles Penetration Mechanics"**, J. Appl. Phys. Vol.37, pp. 1579-1587 (1966)

[15] Tate, A., **"A Theory for the Deceleration of Long Rods After Impact"**, J. Mech. Phys. Solids; Vol. 15, pp.383-399 (1967).

[16] Tate, A., "Further Results in the Theory of LongRods", J. Mech. Phys. Solids, Vol. 17, pp. 141-150 (1969).

[17] Tate, A. **"A Possible Explanation for the Hydrodynamic Transition in High Speed Impacts"**, J. Mech. Sci, Vol. 19, pp. 121-123.

[18] Jones, S.E., P. Gillis and J. foster, Jr. **"On the Penetration of Semi- Infinite Targets by Long Rods"**, J. Mech. Phys. Solids Vol. 35, pp. 121-131 (1987).

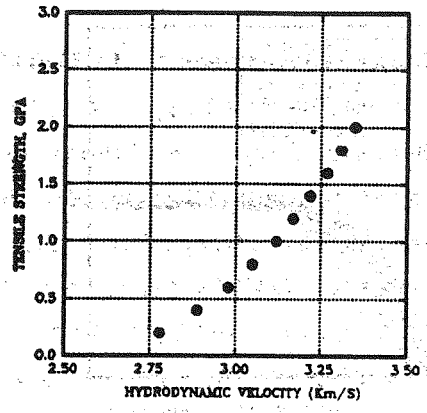

Figure (28)
Effect of Penetrator Strength Variations on Hydrodynamic Velocity

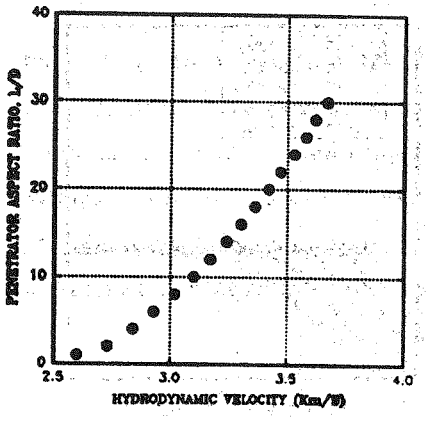

Figure (29)
Effect of Penetrator L/D Variations on Hydrodynamic Velocity

Conclusion

An analytical model was developed for terminal ballistic mechanics in order to predict the crater depth for impacting a cylindrical shape projectile into semi- infinite targets. This study was to take account of strength effects in penetration mechanics and the entire velocity domain has been considered.

The model developed in this paper indicated that hydrodynamic theory can be used at certain velocities to predict the crater depth in an impact event. However at low velocities the hydrodynamic assumption is not valid without certain correction terms. The model also indicated that it is possible to construct a very simple one dimensional model to predict crater depth for a large range of materials and over the entire velocity regime with sufficient accuracy without recourse to high cost experimentation.

Certain assumptions were made in the course of study which should be refined for further study in this respect. Prominent among them are the assumption of initial transient and secondary penetration phase. The conservative prediction of the crater depth in some cases especially at high velocity indicated that this is in fact true and inclusions of these two phases can increase the accuracy of the model. Therefore any further development of this work should include the effect of terminal transient on the model.

The recovery phase was also neglected in this study. Despite its small contribution on the outcome of the problem, this assumption may play some role if highly accurate results are desired.

Another point to consider, is that the formulation of the problem employed the principle of impulse and momentum along with some deduced expression based on assumptions and physical consideration. In fact Equation (19) is a correlational expression which was deduced by comparison with experimental data. Therefore it may require further development and it may not be applicable to all materials in all cases. Also a relation between penetration velocity and rod velocity was assumed which later resulted into an expression for β. This was simply an assumption and there may be better ways to improve this relation. Thus both the resistance

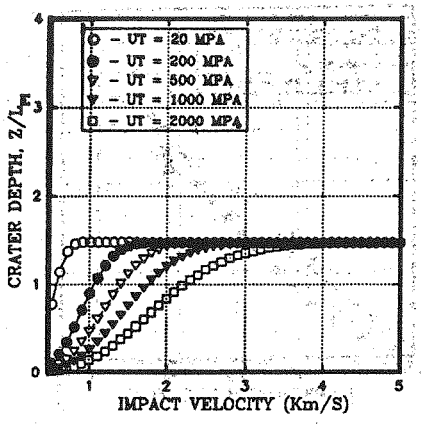

Figure (22)

Effect of Target Tensile Strength on Crater Depth

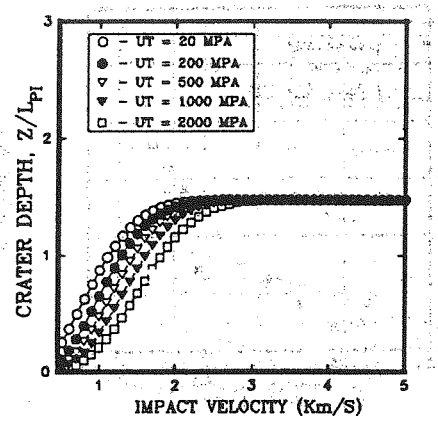

Figure (23)

Effect of Penetrator Tensile Strength on Crater Depth

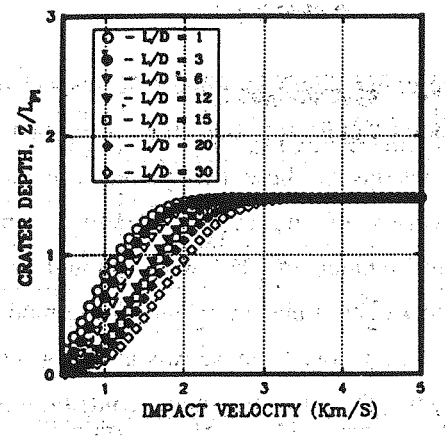

Figure (24)

Effect of Penetrator L/D Variations on Crater Depth

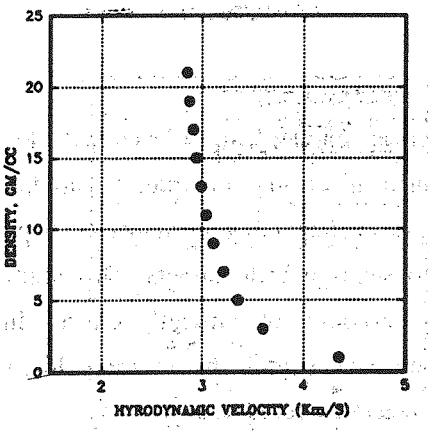

Figure (25)

Effect of Target Density Variations on Hydrodynamic Velocity

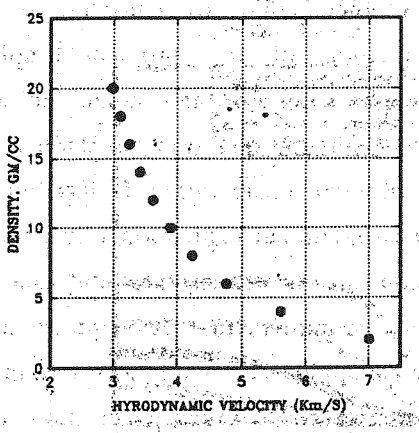

Figure (26)

Effect of Penetrator Density Variations on Hydrodynamic Velocity

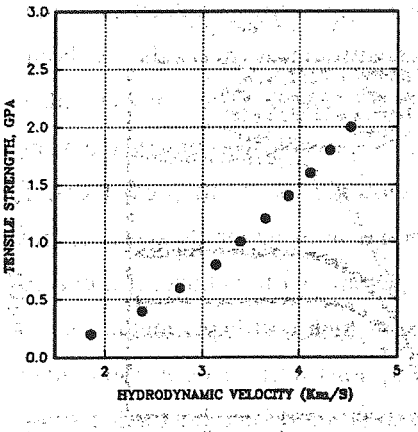

Figure (27)

Effect of Target Strength Variations on Hydrodynamic Velocity

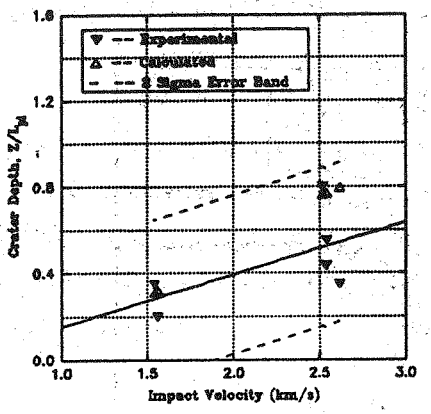

Figure (16)

7075-T6 Aluminum into

7075-T6 Aluminum

L/D=5, Ref. [19]

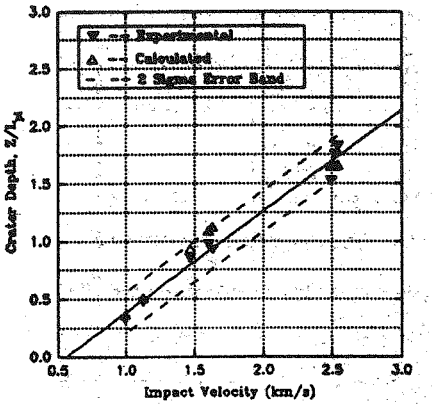

Figure (17)

4340 Annealed Steel into

7075-T6 Aluminum

L/D=5, Ref. [19]

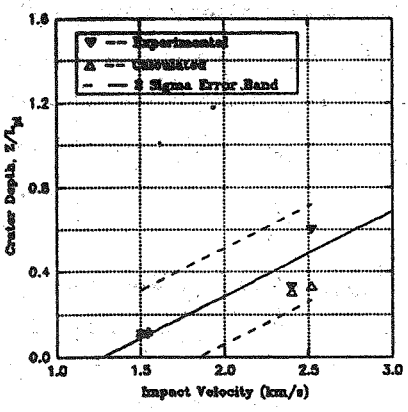

Figure (18)

7075-T6 Aluminum into

4340 Annealed Steel

L/D=5, Ref. [19]

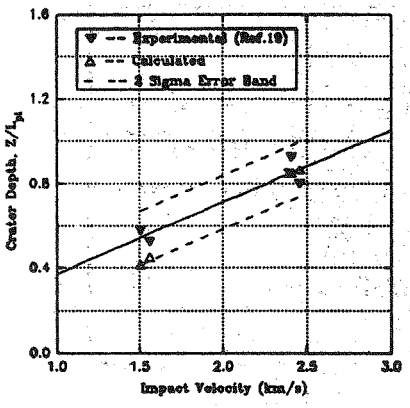

Figure (19)

4340 Annealed Steel into

4340 Annealed Steel

L/D=5, Ref. [19]

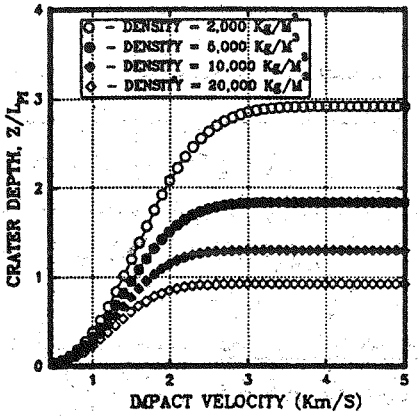

Figure (20)

Effect of Target Density

Variations on Crater Depth

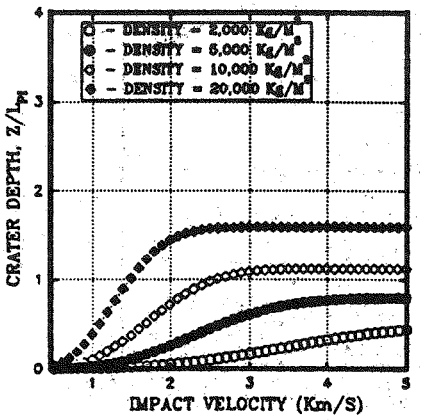

Figure (21)

Effect of Penetrator Density

Variations on Crater Depth

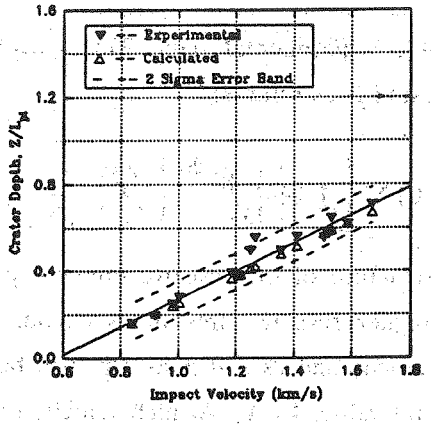

Figure (10)

Steel into Steel

L/D = 3, Ref. [28]

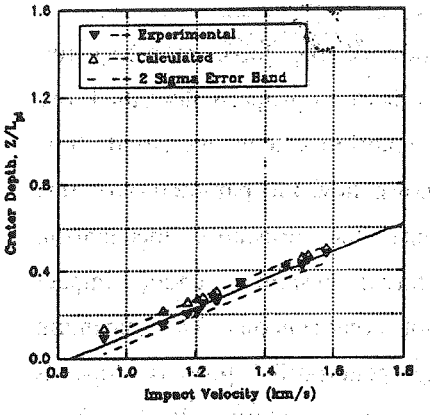

Figure (11)

Steel into Steel

L/D = 6, Ref. [28]

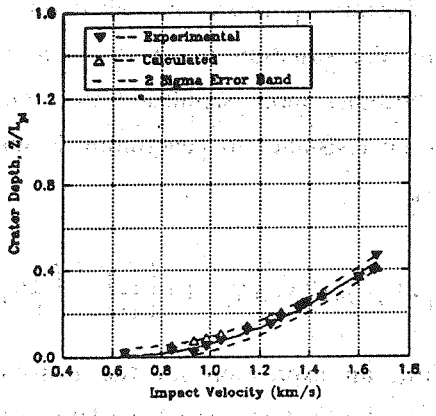

Figure (12)

Steel into Steel

L/D = 12, Ref. [28]

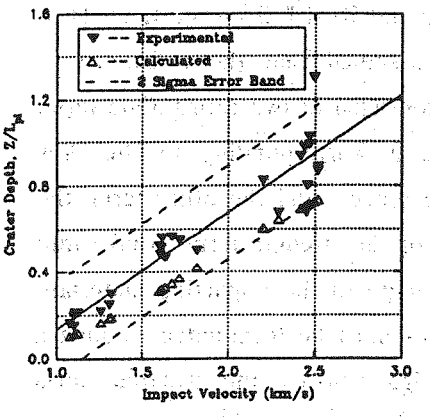

Figure (13)

Hardened Steel into Hardened Steel

L/D = 5, Ref. [19]

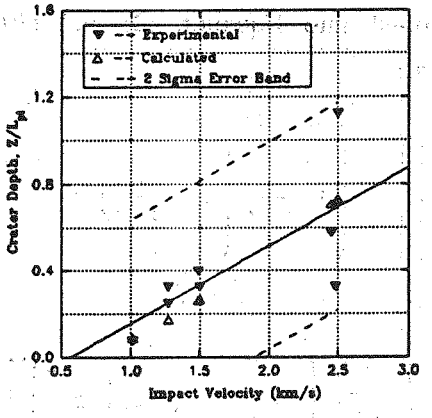

Figure (14)

4340 Annealed Steel into

4340 Hardened Steel

L/D=5, Ref. [19]

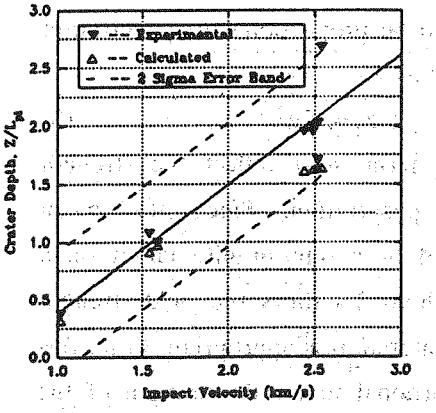

Figure (15)

4340 Hardened Steel into

7075-T6 Aluminum

L/D=5, Ref. [19]

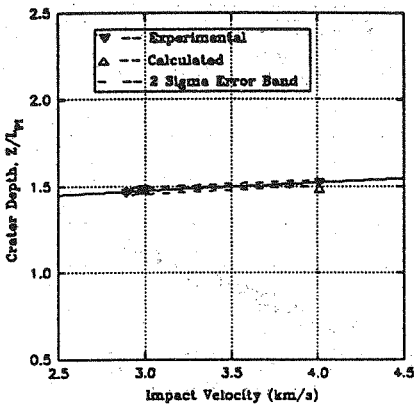

Figure (4)

Tungsten Alloy into RHA

L/D = 15, Ref. [30]

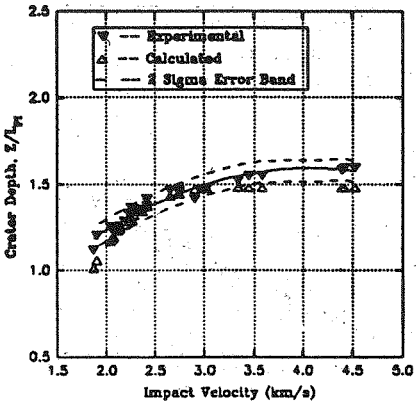

Figure (5)

Tungsten Alloy into RHA

L/D = 20, Ref. [29,30]

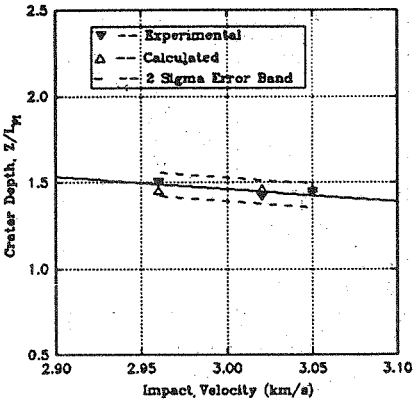

Figure (6)

Tungsten Alloy into RHA

L/D = 30, Ref. [30]

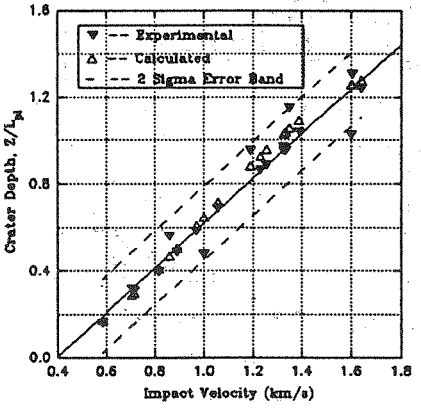

Figure (7)

Tungsten Alloy into RHA

L/D = 3, Ref. [28]

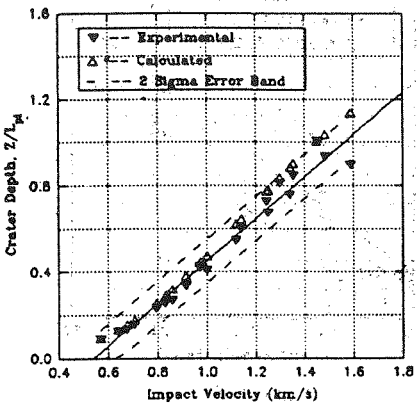

Figure (8)

Tungsten Alloy into RHA

L/D = 12, Ref. [28]

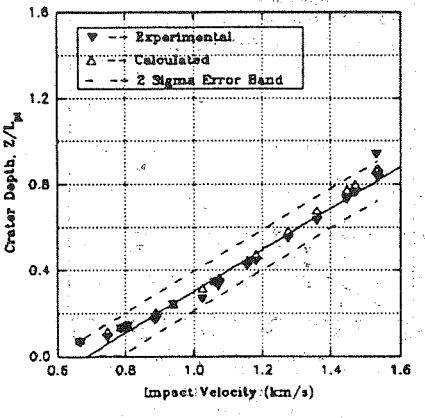

Figure (9)

Tungsten Alloy into RHA

L/D = 6, Ref. [28]

clear definition of hydrodynamic velocity is subject to discussion. There may be some reasons and justifications for this ambiguity. Here attempt is made to signify the effect of variation of penetration parameters on this velocity.

Essentially what has been done here is to vary the parameters of the penetration one at a time and determine the velocity at which penetration depth does not change. 98% of this velocity is assumed to be a valid hydrodynamic velocity. Changing one parameter at a time will determine the effect of that parameter on this velocity. A conclusion and a general result then has been deduced.

The results of the variation of penetration parameters are portrayed in Figures (25) through 29. These figures in principle show what was previously discussed in a more clear an pictorial fashion. For example Figure (25) shows that as the target density increases the hydrodynamic velocity decrease. This effect is more pronounced at low density than at high density. In fact as the density of the target is increased further the resulting change in hydrodynamic velocity is very small. This may be an indication that there is a limit for target material beyond which there is no change in hydrodynamic velocity. It may be concluded that the effect of the target density on hydrodynamic velocity is to lower its value but not beyond a certain point.

Figure (26) shows the effect of penetrator density variation on hydrodynamic velocity. This figure shows the same general pattern but with a lower extant. It may be concluded that penetrator density changes on hydrodynamic velocity is less pronounced than target density changes.

Figure (27) shows the effect of the target strength variation on hydrodynamic velocity. As it is evident from this figure, the target strength has great influence on the hydrodynamic velocity. As the target tensile strength increases hydrodynamic velocity increases and it is evident from the this figure that there is no limit for this situation. Thus it can be concluded that high strength materials require high velocity in order to flow hydrodynamically. This is consistent with what previously perceived but not substantiated with evidence.

Figure (28) is the result of the variation of the penetrator tensile strength on hydrodynamic limit. This situation is completely analogous with target strength variation but with a lesser extant and a general conclusion similar to that can be drawn.

Finally figure (29) shows the effect of penetrator L/D variation on hydrodynamic velocity. This figure shows that as L/D increases the hydrodynamic velocity increase. However if general pattern of the graph is analyzed carefully there appears to be a limit beyond which L/D does not have any effect on hydrodynamic velocity. Once again this is consistent with what was previously discussed concerning the effect of L/D being limited to low velocities.

important result which may not be noticed on first observation. Another point to be mentioned here is that at low velocity the effect of target density variation is not very significant, however as the velocity increases this effect will become very significant as shown in Figure (20).

2. Effect of Penetrator Density Variation

Figure (21) shows the effect of the penetrator density variations on penetration depth. It is clear from this figure that as the density of penetrator increases the crater depth increases pointing to the fact that high density penetrators are more effective than low density penetrators. Comparing Figure (20) and (21) the effect of density variation on target and penetrator are opposite. As far as Hydrodynamic velocity is concerned, the situation is less pronounced in penetrator density variations.

3. Effect of Target Strength Variation

Figure (22) shows the effect of target ultimate yield strength variation on penetration. The figure indicates that changes in the target tensile strength has an enormous effect on determination of the crater depth. As the target strength is increased lower crater depth is predicted. As it is evident from this figure, low strength target is penetrated at relatively low velocity. For low strength case hydrodynamic velocity is higher than for low strength materials. This is a significant result indicating the dependency of the hydrodynamic velocity on target strength.

4. Effect of Penetrator Strength Variation

The effect of penetrator tensile strength variation is reflected in Figure (23). These variations are in contrast to target strength variations. The low strength penetrator tends to penetrate lower into the target and high strength penetrator go deeper into the target. This is consistent with what is expected from a high strength penetrator. High strength penetrators tend to behave more rigidly and therefor penetrate more into the target. For high strength penetrators hydrodynamic velocity is moving to the right showing that higher velocity is required in order for the penetrator to flow hydrodynamically. Comparing the relative significance of target and penetrator strength variation, it is observed that penetrator strength effect is less pronounced than target strength effect as Figure and (22) and (23) show.

5. Effect of Penetrator L/D Variation on Penetration

The effect of penetrator L/D variation on penetration is reflected on Figure (24). Here as the figure shows increasing L/D decreases penetration depth indicating that geometric shape has some effect on determination of the crater depth. This effect is more clear at low velocity than at higher velocity. In fact Figure (24) shows that at hydrodynamic velocity the L/D effect is entirely absent from the process. This result is important because it demonstrates that geometric configuration of the projectile is significant at low velocity only. Another point to be made here is that low L/D penetrators seem to be more effective than high L/D, however one must notice that low length penetrators will be consumed faster.

Parametric Study of Hydrodynamic Velocity

Searching into the literature the boundary and

However these data are valuable in a sense that a large range of aspect ratio is considered (2.5-10) and a general overview of the comparison can be made. The velocity range encompasses from low to high velocities. As it is seen from Figure (12) the calculated results are lower than the experimental results. However the predicted results are almost inside the scatter bands.

Figure (14) show the results of 4340 annealed steel into 4340 hardened steel with aspect ratio of 5. The predicted results are within the scatter bands and the predicted results passes through the center of the data. There is a large scatter in this set of experimental data.

Figure (15) show the results of 4340 hardened steel into 7075-T6 aluminum with aspect ratio of 5. The overall comparison is good except at high velocities in which the predicted results are somewhat lower than experiment. However all the predicted results are within the prescribed bands.

Figure (16) reflect the results of the 7075- T6 aluminum into 7075- T6 aluminum with the aspect ratio of 5. There is an enormous data variation in these data set. Nevertheless predicted results for this case are within the error bands as it is evident from the Figure (15).

Figure (16) show the results of 4340 annealed steel with aspect ratio of 5 impacting into 7075_T6 aluminum. The predicted results are in reasonable agreement with experimental measurements and all the calculated values are within the scatter bands.

Figure (19) is for the results of impacting 7075-T6 aluminum with aspect ratio of 5 into annealed steel. The predicted results are within the 2 sigma line and overall comparison is in a reasonable agreement with experiment.

Figure (19) shows the results of annealed steel into annealed steel. The aspect ratio of the penetrator is 5. Here the overall comparison is good and the predicted results are within the prescribed bands.

Parametric Study

One of the important consideration here is to take account of the variation of the important parameters in penetration. This is being done here to investigate how variation of one parameter will effect the crater depth what general conclusion can be drawn regarding this situation.

The result of this study is useful because it enables one to make an analysis concerning the overall behavior of the penetration mechanics. This procedure is being done by varying one parameter at a time while all the other parameters remained fixed. These results are plotted in Figures (20) through 24.

1. Effect of Target Density Variation:

Figure (20) shows the effect of target density variation on penetration depth. It is seen that as the target density increases lower depth is predicted and hydrodynamic velocity moves to the left. The lower crater depth for high density materials for a given velocity is well indicated in Figure (20). However lower hydrodynamic velocity for higher density materials is indicating that for high density materials this velocity is lower than for low density materials. This does not mean that high density materials are penetrated more than low density materials for a given velocity but indicating that the hydrodynamic velocity for high density materials are lower than high density materials. This is an

Figures (5) shows the results of Tungsten alloy into RHA for aspect ratio of 20. The impact velocity range is high enough for several shots to be considered as hyrodynamical regime. The result of the calculations is a little low with respect to experimental measurements especially for high velocities and for velocities less than 2000 m/s. The low prediction at high velocity is due to the fact that terminal transient (secondary penetration) has been ignored in analytical method. In this high velocity domain, the penetrator was consumed before penetration process was complete. The response of the calculation showed that penetration velocity is still high enough to further penetrate into the target even if all the length of the rod has been consumed. It is evident that this would contribute to the penetration depth in secondary or terminal transient phase of the penetration process. Since initial and terminal transient phases have been neglected in this paper, the results of the calculations are lower than measured experimental data. However the percent difference is not very substantial (less than 8%).

The discrepancies between the predicted results and the experimental data at velocities lower than 2000 m/s may be caused by the resistance formulation Equation (54). This equation is a deduced relation which may predict higher than actual resistance at low velocity causing low penetration depth. Nevertheless over all comparison shows that the difference between the predicted results and the experimental data is less than 10%. Considering the degree of the assumptions involved in analytical approach the predictions are meaningful.

Figure (6) shows the result of the same colliding materials for aspect ratio of 30. As it is evident from the figure the comparison is very good and the difference between the calculated result and the experiment is less than 5%.

Figure (6) through 8 show the results of the tungsten alloy against Rolled Homogeneous Armor (RHA). In these figures three different sets of penetrators have been used. The aspect ratio of the penetrator are 3, 6, 12. Velocity range of the experiments are from 600 to 1600 m/s. It is evident that these regimes are well below hypervelocity range and material properties play a significant role in determining the outcome of the problem. As it is seen from the plotted diagrams the results of the calculations are in good agreement with experimental data. The regression analysis performed on the data to construct 2 sigma error band encompasses all the calculated results in most cases.

Steel Projectile into Steel Target

Figure (9) through 12 show the results of the steel projectiles into steel targets. The velocity ranges are well below hypervelocity cases. The aspect ratio of the penetrator are 3,6,12. The results of the calculations show that the agreement between the calculated results and the experiment are very good indeed. The constructed bands in these figures are encompassing all the calculated results in fact the predicted results pass through the center of data points.

Figure (13) show the results of penetration of 4340 hardened steel into 4340 hardened steel. These data have been extracted from Ref. [19]. Most of the data sets show a considerable amount of experimental data scattering which prevent a valid experimental comparison.

$$- \frac{\rho_t v^2 \left[1 - \frac{\lambda}{1+\lambda} \left(1 - \left(\frac{\gamma}{1+\gamma} \right) e^{-v \left(\frac{\rho_p}{Y_p} \right)^{\frac{1}{2}}} \right) \right]^2}{\rho p^{\ell}} -$$

$$\frac{4.1\, Y_t \left(1 + \left(\frac{L}{D} \right)^{1.26} \left(\frac{Y_p}{\rho_p} \right) \left(\frac{1}{v^2} \right) \right)}{\rho p^{\ell}}$$

Equations (21) and (22) are two equations and two unknowns l and v and can be solved for unique value of each variable. However penetration depth is not included in these equations. Since dZ/dt= u and u is explicitly expressed in terms of v (Eq. 17), calculation of crater depth can be carried out relatively easy.

Solution of the Equations

To solve the above equations the relation dz/dt= u is used to eliminate dt from Equations (21) and (22) and introduce z as the independent variable. The resulting differential equations can be solved very easily using finite difference method.

Now, since

$$\frac{dz}{dt} = u \qquad (23)$$

and since from Equation $u^{(12)} = (1-\beta)\, v$

then

$$\frac{dz}{dt} = (1-\beta)\, v$$

or

$$dt = \frac{dz}{(1-\beta)v} \qquad (24)$$

substituting dt from the above equations into Equations (21) and (22) and simplifying will result into the following equations:

$$\frac{dl}{dz} = - \frac{\beta}{1-\beta} \qquad (25)$$

(26)

$$\frac{dv}{dz} = \frac{v\beta^2}{\ell(1-\beta)} - \frac{\rho_t v [(1-\beta)]}{\rho_p} - \frac{4.1\, Y_t \left(1 + \left(\frac{L}{D} \right)^{1.26} \left(\frac{Y_p}{\rho_p} \right) \left(\frac{1}{v^2} \right) \right)}{v \rho p^{\ell} (1-\beta)}$$

Equations (25) and (26) are the final equations to be solved simultaneously for determination of the crater depth. Since the system is non- linear there is no closed form solution for this system of the equations. Therefore they must be integrated numerically. In order to integrate the above system of equations different methods can be employed, however finite difference method is particularly easy for this situation.

Results

After solving the Equations (25) and (26), the results of the calculations are compared with the experimental investigations. The main sources of comparison are from References [19, 28, 30]. These results are plotted in Figures (3) through 28.In these Figures crater depth Z, normalized with respect to penetrator initial length L_{pi}, are plotted verses impact velocity for various test situations.Aspect ratio (ratio of the length to diameter)of the penetrator is varied from 3 to 30.

Impact of Tungsten Alloy into RHA

Figure (4) shows the results of tungsten alloy into RHA taken from Ref. [30]. The impact velocity is high enough to be taken as hydrodynamic cases. The aspect ratio of the penetrator is 15. The results of the calculations are in very good agreement with experimental data. In fact the percent difference between the calculated and experimentally measured crater depth is less than 5%.

is the formulation of the force retarding the projectile. If this factor is properly described, the accuracy of the solution can be increased. It is not precisely known how the parameters of this problem influence the resistance mechanism. Because the target response under impact conditions is not homogeneous. The maximum pressure during penetration process depends greatly on the target material. It has been estimated that typical pressure and maximum strain rates during penetration may lie in the ranges 5-50 GPa and 10^4-10^6 S^{-1} respectively [12].

Here, it is assumed that the resistance to penetration is consisted of two terms. One term, the dynamic term, corresponding to the flow structure of the process and the other term, the structural term or the strength term to take into account the strength of the impacting materials. These resistances must be formulated in such a way that at high velocity the dynamic term prevails while at low velocity the structural resistance becomes more significant. By analogy with dynamic pressure in fluid mechanics the first term is taken to be proportional to penetration velocity squared as:

$$P_1=\rho_t u^2 \qquad (18)$$

The second term must reflect the strength resistance to penetration. Since the mean pressure exerted by a semi-infinite target on a penetrator is about 3-4 times the yield strength of the target material, it is appropriate to let this term be proportional to tensile strength of the target material. Since the exact expression of the relationship is not known, an expression must be assumed. Once again a great number of possibilities were considered, and the following expression gave reasonably close agreement with available experimental data. This correlational expression is as follows:

$$P_2 = 4.1\, Y_t \left[1 + \left(\frac{L}{D} \right)^{1.26} \left(\frac{Y_p}{\rho_p} \right) \frac{1}{v^2} \right] \qquad (19)$$

The structure of the resistive pressure p_2 shows that higher resistive pressure is encountered at low velocity and as v increases p_2 will become a constant value, 4.1 Y_t. At high velocity this value is negligible compared to p_1 showing that at high velocity structural resistance is less important than dynamic pressure p_1. However at low velocity the situation is reversed and strength term becomes more significant as v decreases. The total resistance to penetration is sum of p_1 and p_2.

$$P = P_1 + P_2 = \rho_t u^2 + 4.1\, Y_t \left[1 + \left(\frac{L}{D} \right)^{1.26} \left(\frac{Y_p}{\rho_p} \right) \frac{1}{v^2} \right] \qquad (20)$$

Now, an expression for the resistance has been deduced, which explicitly relates p in terms of v and other material properties. This expression along with Equation (17) are substituted into Equation (2) and (10). The result is:

$$\frac{d\ell}{dt} = -v \left[1 - \left(1 - \frac{\lambda}{1+\lambda} \left(1 - \left(\frac{\gamma}{1+\gamma} \right) e^{-v \left(\frac{\rho_p}{Y_p} \right)^{\frac{1}{2}}} \right) \right) \right] \qquad (21)$$

$$\frac{dv}{dt} = \frac{\left[\frac{v\lambda}{1+\lambda} \left(1 - \left(\frac{\gamma}{1+\gamma} \right) e^{-v \left(\frac{\rho_p}{Y_p} \right)^{\frac{1}{2}}} \right) \right]^2}{\ell} \qquad (22)$$

To deduce an expression for β the following reasoning based upon the physics of the problem has been employed.

a) At hypervelocities the relationship between u and v should be independent of the strength properties of the target and penetrator.

b) At low velocities the relationship between u and v should depend on the strength properties of the impacting materials.

c) Since l = - (v - u), the higher the xdifference between v and u, the higher the erosion rate. For a given material, higher erosion rate corresponds to higher impact velocity. This translates into the fact that at higher values of impact velocity v, the difference between v and u will be higher. At the same time at low impact velocity, the erosion rate is expected to be low and the difference between v and u decreases to correspond to this situation.

d) In an impact situation, u is expected to depend on the ultimate yieldstrength of the target and penetrator. That is u will be lower if yield strength of the target material is high (imposing more resistance to penetration) and it will be higher if yield strength of the projectile is high (all other conditions unchanged). This is because high strength penetrators tend to behave more like a rigid one and consequently penetrate higher into target.

After considering a great number of possibilities to arrive at a strength dependent expression between these two variables, the following exponential term is considered for β :

$$\beta = \frac{\lambda}{(1+\lambda)}\left[1-\left(\frac{\gamma}{\gamma+1}\right)e^{-v\left[\frac{\rho p}{Y_p}\right]^{\frac{1}{2}}}\right] \quad (13)$$

where λ is the square root of the ratio of the density of the target to the density of the penetrator

$$\lambda = \sqrt{\left(\frac{\rho_t}{\rho_p}\right)} \quad (14)$$

and γ is the ratio of the ultimate yield strength of the target to penetrator.

$$\gamma = \left(\frac{Y_t}{Y_p}\right) \quad (15)$$

The property of this exponential expression is as follows:

1. At hypervelocity the exponential part of the expression for β goes to zero and the relation between u and v becomes independent of the strength properties of the materials and reduces to classical density law.

$$u = \left[1-\frac{\lambda}{1+\lambda}\right] v \quad (16)$$

2. At lower velocity the effect of the strength terms become pronounced as v decreases. The value of β increases as the difference between u and v decreases corresponding to the fact that at low velocity erosion rate becomes smaller and smaller. The relationship between u and v in this situation is Equation (17) which expresses u directly in terms of v and other material properties and can be used into Equations (2) and (10) to eliminate u.

Now we proceed to determine an expression for p in terms of v and other

$$u = v\left[1-\frac{\lambda}{1+\lambda}\left(1-\left(\frac{\gamma}{1+\gamma}\right)e^{-v\left(\frac{\rho_p}{Y_p}\right)^{\frac{1}{2}}}\right)\right] \quad (17)$$

properties of the materials.

2. Resistance Formulation

The main difficulty in penetration mechanics

The internal force F_i's are equal and opposite and only the external force F contributes to the impulse. The expression for F is not known at the moment and will be specified below. Also, F during Δt is a variable. By considering a quasi-steady state an expression for F is obtained. Since the direction of F is opposite to that of u and v its contribution is negative, which indicates that the penetrator will encounter a resistive force opposite to that of penetrator motion. Since the rod is decelerating Δv is negative, however the loss of mass tends to accelerate the penetrator and counteract the target resistive force.

In these equations mass dM has been lost from the front portion of the projectile while the speed of the back of the rod becomes v - dv.

The above equation can be reduced into the following form

$$\rho_p A \left[(L-X) \frac{dv}{dt} - \frac{dX}{dt} (v - u) \right] = F \qquad (5)$$

Now, since ℓ was defined to be equal to L-X, then

$$\dot{\ell} = - \dot{X} \qquad (6)$$

Substituting equation (6) into equation (5)

$$\rho_p A \left[\ell \frac{dv}{dt} + \dot{\ell}(v - u) \right] = F \qquad (7)$$

And substituting Equation (2) into (7) gives:

$$\rho_p A \left[\ell \frac{dv}{dt} - (v - u)^2 \right] = F \qquad (8)$$

Dividing both sides of equation (8) by $\rho_p A$ and solving for dv/dt:

$$\frac{dv}{dt} = \frac{(v - u)^2}{\ell} + \frac{F}{\rho \ell A} \qquad (9)$$

and finally noting that the average interface pressure P=-F/A

$$\frac{dv}{dt} = \frac{(v - u)^2}{\ell} - \frac{P}{\rho_p \ell} \qquad (10)$$

Equation (10) is the equation for the deceleration of the rod, knowing that p, the resistance pressure, must be properly specified. Equations (2) and (10) are two equations and four unknowns; u, v, p and ℓ.

If P and u are can be explicitly expressed in terms of v and material properties of impacting objects then these two variables can be eliminated from Equations (2) and (10) and the system can be solved for a unique value of each variable namely v and ℓ. This is what needs to be done.

Relational Development Among Variables

At this point a mathematical expressions relating p and u in terms of v and other material properties is developed.

In order to express u in terms of v and other material properties, it is assumed that erosion rate, $\dot{\ell}$, is proportional to instantaneous rod velocity. And since u and v are coupled by equation (2) u can be expressed in terms of v. Employing this concept, the following relation is assumed between v and ℓ:

$$\dot{\ell} = - \beta v \qquad (11)$$

where β is a proportionality parameter relating v and u and depending on the physical properties of the impacting materials. Using the above assumption along with Equation (2)

$$\ell = (u\text{-}v)$$

will result in

$$u = v (1\text{-}\beta) \qquad (12)$$

Equation (12) explicitly expresses u in terms of v if the dependency of β on material properties is established. If β is taken to be a constant, then the question of what value should be assigned to it poses a problem even though Equation (12) indicates that the limits of β are between 0 and 1. On the other hand it is highly probable that β is not a constant.

In order to properly specify β, the penetration process should be analyzed carefully.

undeformed section of the rod is preserved we can write

$$\dot{M} = \rho_p \dot{\ell} A \qquad (1)$$

It is noted that the undeformed portion of the rod may not preserve its shape before erosion and some of the resistive pressure will cause deformation in that part. Although the detailed analysis of the error of introducing this assumption has not been carried out it is assumed that this does not introduce significant error in achieving the prime goal of the problem which is to predict penetration depth. It is to be noted that because of the tremendous pressure generated in the undeformed part of the rod due to compression waves, remaining length of the rod after penetration (if any) may be distorted depending on material characteristics of the penetrator.

2. Rod Erosion Rate

The rate of decrease of the rod length with respect to time is defined as the erosion rate. Assuming that the deceleration is finite this quantity is obtained in the following manner:

During time interval Δt, the nose end of the penetrator will move a distance $u.\Delta t$ while the rigid part of it will move a distance equal to $v.\Delta t$. So the change in length of the rod will be $\Delta \ell = u.\Delta t - v.\Delta t$ where u is the instantaneous penetration velocity and v is the instantaneous speed of the undeformed portion of the rod. Dividing both sides of this equation by Δt and taking the limit as Δt approaches zero we obtain the following equation which is a relationship between variables u,v and ℓ

Thus the velocities u and v are coupled by the above kinematical relationship. Comparing Equations (1) and (2) we can write:

$$\dot{\ell} = -(v - u) \qquad (2)$$

$$\dot{M} = -(v - u)\rho_p A \qquad (3)$$

or

$$u = v + \frac{\dot{M}}{\rho_p A} \qquad (4)$$

which indicates that u is less than v, since M is negative. Whenever the erosion rate, M, is zero, u will be equal to v, that is, we have rigid body penetration.

3. Rod Deceleration Equation

Now applying the principle of impulse and momentum to a cylindrical projectile of length L-X and cross sectional area, A, as shown in Figure 3, the following relation can be written for the undeformed portion of the rod.

Momentum at time t + Δt - Momentum at time t = F Δt

where $\rho_p A$ (L-X) v = **Momentum at time t**

$\rho_p A$ (ΔX) u + $\rho_p A$ (L-X-ΔX) ($v+\Delta v$) = **Momentum at time t+Δt**

and $F\Delta t$ = **Impulse**

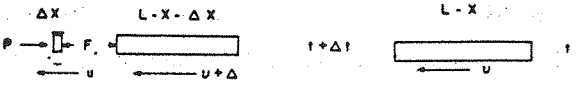

Figure(3)Schematic of the transfer of mass element $\rho_p A\Delta X$ from the undeformed to the plastic portion of rod.

3. Cavitation Regime

After the projectile has been completely eroded or has been stopped in the penetration process the crater continues to expand under its own inertia. This third regime, the so called second penetration phase or terminal transient, continues until the energy density of the material surrounding the crater becomes too small to overcome the intrinsic resistance to deformation of the material. The second and third phases may actually exist simultaneously in a target.

4. Recovery Regime

The forth regime or recovery phase is defined as the period during which recovery or contraction of the crater takes place. In this phase the final crater size may actually decrease and become smaller than the maximum size achieved at the end of secondary phase

Formulation of the Problem

The following assumptions are used in order to formulate the problem.

a) Transient phenomena is neglected. (it is assumed that penetration process starts when the resistive forces have peaked).

b) Terminal transient is ignored

c) Recovery phase is assumed to be negligible.

d) Target resistance to penetration is a variable quantity depending on striking velocity, target tensile strength, diameter and length of the penetrator.

e) The target/ penetrator interaction is principally one dimensional for determination of crater depth.

f) Heat transfer is assumed negligible.

Now, a cylindrical projectile having an initial length of L and penetrating into a semi- infinite target is considered. The density of the rod is denoted by ρ_p and the area of its cross section by A, such that $M=\rho_p \ell A$ is its mass at any time after the impact, where ℓ is the length of the undeformed rod at any time. The rod material can be separated into rigid and plastic regions during the penetration process. Depth of penetration is denoted by Z. The undeformed length, ℓ, can be seen to be equal to L-X where X is the length of the consumed part of the rod as shown in Figure (2).

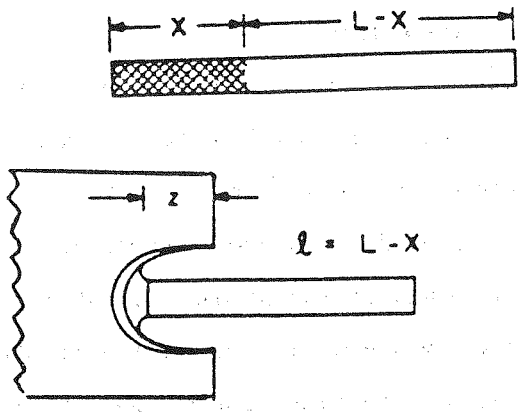

Figure (2) Schematic of rod showing plastic portion X and undeformed portion ℓ=L-X along with penetration depth, z.

During the penetration process, the rod will erode, deform, and penetrate into the target. Assuming that the cylindrical shape of the

b) Nominal Ordnance Range- As the impact velocity increases to 500- 1300 m/s, the response of the structure becomes limited to a small zone of impact area (usually 3-4 times projectile diameter). A wave description of the phenomena is appropriate. Typically, loading and reaction times are on the order of a few hundred microseconds.

c) Ultra Ordnance Domain- As the velocity increases further to 1300-3000 m/s the localized pressure will exceed the strength of the materials by an order of magnitude. In effect the colliding materials can be treated as plastic flow. Loading and reaction times are on the order of a hundred microseconds for this velocity regime.

d) Hypervelocity Regime- Velocity regimes greater than 3000 m/s are often considered to be high enough for the solid materials to behave as inviscid fluids. The strength of the colliding materials are ignored in the analysis of this situation. The above velocity regimes are approximate in nature and a typical material behavior may not correspond to the above divisions.

Theoretical Background

The pressure history generated at the interface between the projectile and the target in usually divided into four separate regimes as follows [7].

1. Transient Shock Regime

The first or transient phase begins when the projectile first contacts the target and lasts for only a brief period of time of the order of a few microseconds. Figure (1). on a qualitative bases shows a high pressure spike in first phase.

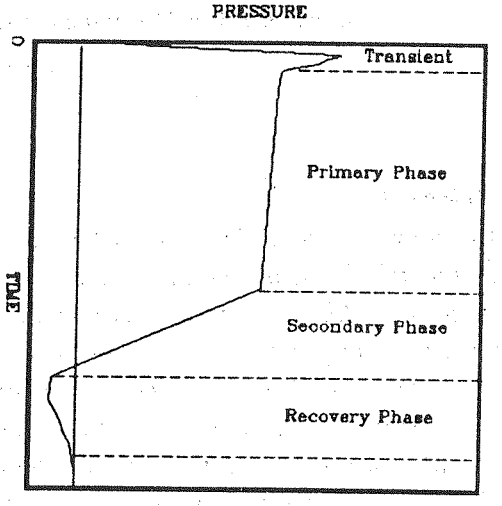

Figure (1) Schematic representation of the four phases of high velocity penetration.

2. Primary Penetration Phase

After several reflections of rarefaction waves in the projectile which release the very high initial pressure, a condition of steady flow is established, during which the projectile which is steadily eroded, and the crater is being formed. The duration of this regime, the steady state regime, is based upon the relation of length of the projectile to its diameter, and for a short projectile may be entirely absent.

However, for long rod penetrators at hypervelocity range this phase is the dominant one. During this stage the crater is deepened at a constant speed.

Development of an Analytical Model for Ballistic Impact of Long Rod Penetrators

Khodadad Vahedi

Department of Mechanical and Industrial Engineering Louisiana Tech University, Ruston La.

U.S.A

ABSTRACT:

An analytical model in terminal ballistic is developed to predict the crater depth of a projectile impacting into a semi- infinite target. A principal objective was to take account of strength properties of colliding materials. The entire velocity regime from low to hypervelocity is analyzed. The model developed here is based on steady state penetration process, and is used to compare with existing experimental measurements. The study shows that it is possible to construct a very simple model to predict crater depth for a large range of materials with sufficient accuracy without recourse to high cost of experimentation. In fact the biggest advantage of this model is simplicity and direct applicability to design process. Penetration mechanics has relied heavily on high cost experimental investigation. This work gives a quick and easy result with sufficient accuracy which may be useful for many applications. This work further demonstrates that classical approaches which neglect strength properties are inadequate in describing penetration mechanics and have limited applicability specially at low velocities.

Introduction

Situations involving the collision of two or more solids occur in numerous engineering disciplines. The study of terminal ballistic mechanics involves a variety of disciplines and a complete description of the dynamics of impacting solids would demand that consideration be given to the geometry of the interacting bodies, elastic, plastic, and shock wave propagation, hydrodynamic flow, finite strain and deformation, work hardening, thermal and frictional effects and the initiation and propagation of failure in the colliding materials. The presence of all the above factors constitute a formidable obstacle for an analytical approach in terminal ballistics. Terminal ballistics is usually divided into several velocity regimes in order to facilitate analysis as follows [1,2]:

a) Low Velocity Regime- Impact velocities less than 500 m/s are considered to be low in the low velocity regime. In this regime many problems fall into the area of structural dynamics. Local indentations or penetrations are strongly coupled to the over-all deformations of the structure. Typically, loading and response times are of the order of a millisecond in this regime.